Cite this: *Dalton Trans.*, 2018, 47, 1726

Effect of coordination geometry on the magnetic properties of a series of Ln_2 and Ln_4 hydroxo clusters†

Amaleswari Rasamsetty,[a] Chinmoy Das,[b] E. Carolina Sañudo,[c] Maheswaran Shanmugam *[b] and Viswanathan Baskar *[a]

A series of three isostructural tetranuclear complexes with the general molecular formula [$Ln_4(\mu_3$-$OH)_4(L)_4(\mu_2$-$piv)_4(MeOH)_4$] (Ln = Gd 1, Dy 2 and Ho 3; LH = [1,3-bis(*o*-methoxyphenyl)-propane-1,3-dione]) were isolated and unambiguously characterized by single crystal XRD. Under similar reaction conditions, simply changing the co-ligand from pivalate to 2,6-bis(hydroxymethyl)-*p*-cresol (LH'_3) led to the isolation of dinuclear Ln(III) complexes with the general molecular formula [$Ln_2(L)_4(\mu_2$-$LH'_2)_2$]·4DMF (Ln = Gd 4, Dy 5 and Ho 6). Direct current magnetic susceptibility data studies on the polycrystalline sample of 1–6 and the results reveal the existence of weak antiferromagnetic exchange interactions between the lanthanide ions in 1 which is evident from the spin Hamiltonian (SH) parameters (J_1 = −0.055 cm^{-1} and g = 2.01) extracted by fitting $\chi_M T(T)$. On the other hand, though complex 4 exhibits weak antiferromagnetic coupling (J_1 = −0.048 cm^{-1} and g = 1.99) between the Gd(III) ions, the $\chi_M T$ (T) data of complexes 5 and 6 unambiguously disclose the presence of ferromagnetic interactions between Dy(III) and Tb(III) ions at lower temperature. Magnetization relaxation dynamics studies performed on 2 show frequency dependent out-of-phase susceptibility signals in the presence of an optimum external magnetic field of 0.5 kOe. In contrast, complex 5 shows slow magnetization relaxation with an effective energy barrier (U_{eff}) of 38.17 cm^{-1} with a pre-exponential factor (τ_0) of 1.85 × 10^{-6} s. The magnetocaloric effect (MCE) of complexes 1 and 4 was extracted from the detailed magnetization measurement and the change in the magnetic entropy ($-\Delta S_m$) of 1 and 4 was found to be 25.57 J kg^{-1} K^{-1} and 12.93 J kg^{-1} K^{-1}, respectively, at 3.0 K for ΔH = 70 kOe.

Received 16th January 2017,
Accepted 6th December 2017

DOI: 10.1039/c7dt00172j

rsc.li/dalton

Introduction

Multinuclear lanthanide clusters have become very important in recent years owing to their intriguing and interesting magnetic properties and their application as single molecule magnets (SMMs)[1] and molecular magnetic coolants.[2] Discrete molecules which exhibit slow relaxation of magnetization below a certain temperature (blocking temperature, T_B) are referred to as single molecule magnets. The unquenched orbital angular momentum in lanthanide complexes makes them an ideal candidate to reveal a new generation of SMMs compared to transition metal complexes. In fact, this has been proven successful recently in a two coordinated Dy(III) complex with a record blocking temperature of 60 K.[1l] Moreover, apart from SMM behaviour, larger oligomeric clusters were observed to show other fascinating physical phenomena such as single molecule tri,[4] tetra (linear, grids, cubanes, rhombus, Y-shaped, seesaw),[5] and polynuclear[6] clusters] have been reported to identify such suitable molecules, so as to envisage molecule based devices. Although

several approaches exist in the literature to modulate U_{eff} (whereby T_B), studies on the influence of substituents on the ligand, and on the magnetization relaxation dynamics of lanthanide ions, are extremely rare in the literature. For example, Murugesu and co-workers[7] have recently investigated such a phenomenon. β-Diketones' coordination potential has been extensively studied in the literature,[11] due to their preferential bidentate chelating mode.[8–10] However, reports pertaining to investigations of the coordination potential of functio-

[a]*School of Chemistry, University of Hyderabad, Hyderabad 500046, India*
[b]*Department of Chemistry, Indian Institute of Technology Bombay, Mumbai, 400076, India. E-mail: eswar@chem.iitb.ac.in*
[c]*Departament de Química Inorgànica i Institut de Nanociència i Nanotecnologia, Universitat de Barcelona, Diagonal 645 08028, Barcelona, Spain*

†Electronic supplementary information (ESI) available: Molecular structure of 1, 3, 4 and 6, shape calculation table, and selected metric parameters for 1–6. CCDC 1523360–1523365. For ESI and crystallographic data in CIF or other electronic format see DOI: 10.1039/c7dt00172j

nalized β-diketones are rare in the literature.[4a,12] In addition to SMMs, magnetic refrigeration exhibited by lanthanide clusters is also being increasingly investigated. The magnetic cooling efficiency was evaluated in terms of its intrinsic magnetocaloric effect, *i.e.*, the change in the temperature of the material with the aid of an external magnetic field. Isotropic molecular clusters are potentially targeted as magnetic coolants, which could be a suitable alternative to cryogenic liquid ^{3}He to achieve ultralow temperatures.[13] Change in magnetic entropy ($-\Delta S_m$) and change in temperature (ΔT_{ad}) are the two parameters which quantify the MCE of a particular cluster. High magnetic density (high metal to ligand ratio),[14] negligible magnetic anisotropy (preferably isotropic in nature) and spin degeneracy are the key factors which play a pivotal role in determining the MCE of clusters. The large spin ground state, negligible magnetic anisotropy, high magnetic density and weak ferromagnetic interactions associated with polymetallic Gd(III) complexes with suitable organic ligands make them behave as magnetic coolants.

With the aim of revealing a new generation of SMMs and magnetic coolants, the use of the bisortho-methoxy functionalized β-diketone (LH) ligand along with other co-ligands for the synthesis of Ln(III) clusters was investigated. The use of LH and pivallic acid (pivH as a co-ligand) resulted in successful isolation and characterization of three new tetranuclear clusters with a distorted cubane core with the general formula $[Ln_4(\mu_3\text{-}OH)_4(L)_4(\mu_2\text{-}piv)_4(MeOH)_4]$ (Ln = Gd 1, Dy 2, Ho 3). Similarly, changing the pivallic acid (pivH) to a bulky co-ligand 2,6-bis(hydroxymethyl)-*p*-cresol (LH_3) resulted in the isolation of three new dinuclear Ln(III) complexes with the general formula $[Ln_2(L)_4(\mu_2\text{-}LH'_2)_2]4CH_3CN/DMF$ (Ln = Gd 4, Dy 5 and Ho 6) and their magnetic properties have been studied in detail.

Results and discussion

A reaction between β-diketone (LH), pivH or LH_3' and the corresponding $LnCl_3{\cdot}xH_2O$ (Ln = Gd or Dy or Ho) in methanol afforded neutral tetranuclear $[Ln_4(\mu_3\text{-}OH)_4(L)_4(\mu_2\text{-}piv)_4(MeOH)_4]$ (Ln = Gd 1, Dy 2 and Ho 3) and dinuclear $[Ln_2(L)_4(\mu_2\text{-}LH'_2)_2]$ $4CH_3CN/DMF$ (Ln = Gd 4, Dy 5 and Ho 6) lanthanide(III) complexes in good yields (60–65%).

Structural description

Compounds 1–3. Single crystal X-ray diffraction analysis revealed the structure of all the three complexes with the general molecular formula $[Ln_4(\mu_3\text{-}OH)_4(L)_4(\mu_2\text{-}piv)_4(MeOH)_4]$ (Ln = Gd 1, Dy 2 and Ho 3). All the three complexes are crystallized in the monoclinic space group $P2/n$ which are structurally analogous to each other. This is further strongly corroborated by their unit cell parameters (Table 1). Due to their structural similarity, 2 is chosen as a prototype for discussion. The crystal structure of 1 and 3 is given in the ESI (Fig. S1 and S2†). The molecular structure of 2 is depicted in Fig. 1. Complex 2 is a tetrameric cluster and all the Dy(III) ions occupy the alternate corners of a distorted cube. The asymmetric unit consists of two crystallographically distinct Dy_2-half units and hence one unit of these is considered for detailed discussion. As far as the constituents of this unit are concerned, it consists of a hydroxo bridged dysprosium dimer coordinated by two β-diketones, two pivallic acids and two methanol molecules. Bridging oxygen atoms O_{10} and O_{11} of μ_3-hydroxy groups gen- erates the full cluster (distorted cubane motif). Overall, the cubane core is surrounded by four β-diketonates and four pivalates. Each β-diketonate binds to the metal in a chelating mode and further the cubane core is held together by four pivalate ligands. Each pivalate ligand binds to the metal in a

Table 1 Crystallographic data and structure refinement for 1–6

	1	2	3	4	5	6
Empirical formula	$C_{92}H_{116}O_{32}Gd_4$	$C_{92}H_{116}O_{32}Dy_4$	$C_{92}H_{116}O_{32}Ho_4$	$C_{98}H_{106}N_4O_{26}Gd_2$	$C_{98}H_{106}N_4O_{26}Dy_2$	$C_{98}H_{106}N_4O_{26}Ho_2$
F_w g mol^{-1}	2362.85	2383.85	2393.57	2070.36	2080.87	2085.73
Crystal system	Monoclinic	Monoclinic	Monoclinic	Triclinic	Triclinic	Triclinic
Space group	$P2/n$	$P2/n$	$P2/n$	$P\bar{1}$	$P\bar{1}$	$P\bar{1}$
a/Å	25.191(4)	25.136(5)	25.118(3)	13.868(6)	13.859(12)	13.8538(14)
b/Å	14.292(3)	14.190(3)	14.1850(14)	13.939(6)	13.906(12)	13.8879(14)
c/Å	27.482(5)	27.383(5)	27.365(3)	15.1576(6)	15.079(12)	15.0749(15)
α (°)	90	90	90	64.652(2)	64.692(10)	64.6480(10)
β (°)	101.401(3)	101.308(10)	101.334(2)	64.498(2)	64.850(10)	64.9470(10)
γ (°)	90	90	90	85.951(2)	85.947(10)	85.963(2)
v/Å	9699(3)	9577(3)	9560.0(17)	2366.7(18)	2356.3(4)	2352.6(4)
Z	4	4	4	1	1	1
ρ_c/Mg m^{-3}	1.618	1.653	1.663	1.453	1.466	1.472
μ/mm^{-1}	2.778	3.165	3.354	1.467	1.652	1.748
F(000)	4720	4752	4768	1058	1062	1064
θ range (°)	1.00 to 24.77	1.23 to 25.00	1.01 to 25.09	2.149 to 27.612	1.63 to 25.06	1.64 to 25.02
Reflns collected	89 512	90 520	91 105	140 134	22 854	22 692
Completeness to θ (%)	99.7	99.9	99.7	99.9	99.5	99.4
Ind refln/R_{int}	16 610/0.0550	16 853/0.0391	16 947/0.0996	10 960/0.0424	8327/0.0335	8264/0.0266
GooF(F^2)	1.051	1.072	1.111	1.051	1.047	1.045
Final R indices ($I > 2\sigma(I)$)	$R_1 = 0.0366$	$R_1 = 0.0360$	$R_1 = 0.0588$	$R_1 = 0.0182$	$R_1 = 0.0303$	$R_1 = 0.0266$
	w$R_2 = 0.0887$	w$R_2 = 0.0849$	w$R_2 = 0.1100$	w$R_2 = 0.0448$	w$R_2 = 0.0741$	wR_2 = 0.0679
R indices (all data)	$R_1 = 0.0430$	$R_1 = 0.0398$	$R_1 = 0.0783$	$R_1 = 0.0206$	$R_1 = 0.0323$	$R_1 = 0.0274$
	w$R_2 = 0.0922$	w$R_2 = 0.0869$	w$R_2 = 0.1173$	w$R_2 = 0.0457$	w$R_2 = 0.0752$	wR_2 = 0.0684

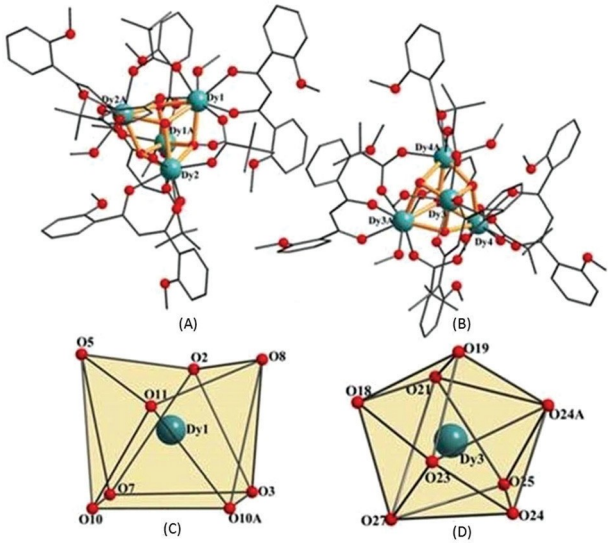

Fig. 1 (A) Crystal structure of the two crystallographically distinct molecules present in the crystal lattice of 2 (C) the square prism geometry around Dy(III) ions in molecule 1 present in panel A. (D) The trinangular dodecahedron geometry (TDD) around the Dy(III) ion in molecule 2 represented in panel B.

syn–syn bridiging mode μ_2–η^1:η^1. Each Dy(III) ion is octa-coordinated with 3 μ_3-OH anions, 2 oxygen atoms from the β-diketonate ligand, 2 oxygen atoms from pivalic acids and finally the coordination is completed by a methanol molecule.

The systematic analysis of the coordination geometries around the metal atoms using SHAPE 2.1 [15] reveals that the octa-coordinated metal ions Dy1(III) and Dy2(III) adopt dis- torted square antiprismatic (SAP) geometry with the *pseudo* D_{4d} symmetry (Fig. 1C) (with skew angle 39.5°). Though a similar bonding perspective is observed for another asym- metric unit in the crystal lattice, the Dy(III) ions in this mole- cule exhibit triangular dodecahedron (TDD) geometry with the D_{2d} symmetry (Fig. 1D) which rationalizes the presence of two crystallographically distinct Dy_2-half units in the unit cell of all the complexes (1–3). The complete results of geometric analysis are described in the ESI (Table S1†). The Dy–O(diketone) and Dy–O(piv) bond lengths are in the range of 2.35–2.37(3) Å and 2.29–2.33(3) Å, respectively. Dy–Dy distances are in the range of 3.74–3.83(7) Å and Dy–$O_{(\mu_3\text{-OH})}$ distances are in the range of 2.35–2.38(3) Å. The Dy–O–Dy angles are of the order of 104.54–108.51(12)° which is close to the tetrahedral geometry and the O–Dy–O angles are in the range of 69.22–144.29(12)° due to the geometrical strain. All the bond lengths and bond angles observed in complexes 1–3 are similar to the other cubane motifs reported in the literature (Table S2†).[16]

Compounds 4–6. When the reaction was carried out under similar conditions to isolate complexes 1–3 (except that LH_3 was used instead of pivalic acid), single crystals related to another series of complexes (4–6) were obtained from a DMF/MeOH solvent mixture. Structure elucidation reveals the general molecular formula of these complexes as $[Ln_2(L)_4(\mu_2\text{-}LH'_2)_2]$4DMF (Ln = Gd 4, Dy 5 and Ho 6). Like 1–3, complexes

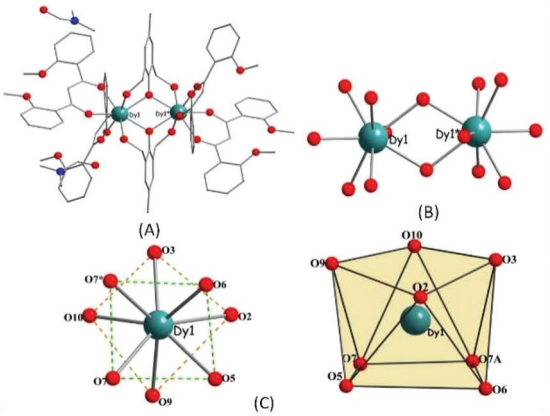

Fig. 2 (A) Molecular structure of compound 5 (B) represents the core of the cluster (C) coordination geometry around Dy(III) ions.

4–6 are structurally analogous to each other and exist as a dimer (Table 1). Owing to their structural similarity, dysprosium analogue 5 is chosen for discussion (Fig. 2, see also Fig. S3 and 4†). All the three complexes crystallized in a triclinic, $P\bar{1}$ space group (Table 1). Only half of the molecule presents as an asymmetric unit and the remaining fragment of the molecule is generated by symmetry operation (inversion center). In the asymmetric unit, the Dy(III) ion is surrounded by eight oxygen donors which are derived from two chelating β-diketonates, two alkoxy oxygen atoms of LH′3 and two phenoxy oxygens of LH′3. The Dy–$O_{(diketone)}$, Dy–$O(alkoxy_{LH_3})$ and Dy–$O_{(phenoxyLH_3)}$ bond lengths are of the order of 2.301–2.343(2) Å, 2.313–2.438(2) Å and 2.313–2.438(2) Å, respectively. The two Dy(III) ions in 5 (as well as in 4 and 6) are exclusively bridged by the phenoxy oxygen atom of LH′3 and the bond angle is found to be ∠Dy1–O6–Dy1* = 113.81°. The octa-coordinated Dy(III) ion exists in the distorted square antiprism (with skew angle 39.5° which is slightly deviated from the ideal value 45° for SAP) geometry with the *pseudo* D_{4d} symmetry which was confirmed by using CShM software[22] [Fig. 2(c), Table S1†]. The two dysprosium centers are separated by an intramolecular distance of 3.882(3) Å. Selected bond distances and bond angles for all the compounds are given in the ESI (Table S3†).

Magnetic properties

Static magnetic susceptibility. Variable temperature dc magnetic susceptibility data were collected for all the complexes at 1 kOe applied field from 300 to 2 K. The $\chi_M T$ as a function of temperature plot is shown in Fig. 3(A) for the complexes 1–3. The observed room temperature $\chi_M T$ values of 31.41 (1), 55.12 (2) and 52.60 cm^3 K mol^{-1} (3) are slightly lower than the expected values of 31.5 cm^3 K mol^{-1} (g = 2.0; S = 7/2; L = 0, $^8S_{7/2}$ for 1), 56.67 cm^3 K mol^{-1} (g = 4/3; S = 5/2; L = 5; $^6H_{15/2}$ for 2), and 56.25 cm^3 K mol^{-1} (g = 5/4; S = 2; L = 6; $^5I_8$ for 3) for magnetically dilute Gd(III), Dy(III) and Ho(III) ions, respectively (Table 2). The $\chi_M T$ value for 1 remains constant from room temperature to T = 45 K below which it steadily decreases

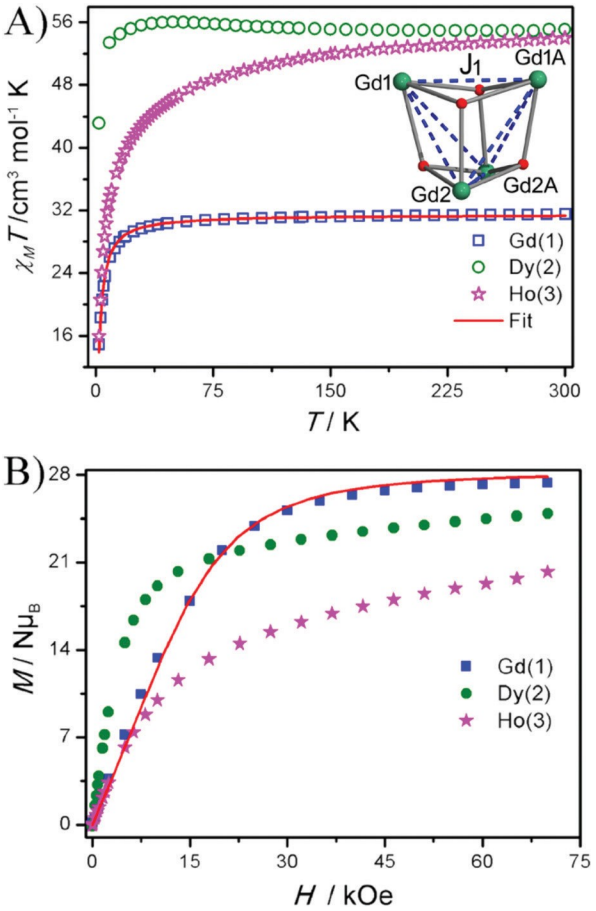

Fig. 3 (A) Temperature dependence of the product of magnetic susceptibility and temperature ($\chi_M T$) for 1–3 measured in the presence of 1 kOe. The red solid line represents the best fit obtained for the $\chi_M T$ data of 1 using the parameters described in the main text. A inset: A model depicts the number of exchange used to model the magnetic data of 1. (B) Field dependent magnetization measurement performed on the polycrystalline sample of 1–3 at 2 K. The solid line represents the simulation of the magnetization data of 1 using the parameters extracted from $\chi_M T$ data fitting.

Table 2 Calculated and observed $\chi_M T$ values for 1–6 at room temperature

					$\chi_M T$ at room T (cm^3 K mol^{-1})	
	S	L	J	g	Expected	Experimental
1	7/2	0	7/2	2	31.50	31.41
2	5/2	5	15/2	4/3	56.67	55.12
3	2	6	8	5/4	56.25	52.60
4	7/2	0	7/2	2	15.75	17.41
5	5/2	5	15/2	4/3	28.34	28.62
6	2	6	8	5/4	28.13	27.65

before precipitously falls below 35 K to a value of 14.89 cm^3 K mol^{-1} at 2.0 K. The $\chi_M T$ value for 3 gradually decreases from room temperature to T = 55 K, likely due to the depopulation of m_J levels. The $\chi_M T$ value drops rapidly below 45 K and reaches a value of 15.93 cm^3 K mol^{-1} (for 3).

In contrast, for 2, the $\chi_M T$ value remains constant in the entire temperature range from room temperature to 42 K; upon decreasing the temperature further, the $\chi_M T$ value of 2 decreased rapidly and reaches a value of 43.2 cm^3 K mol^{-1} at 2 K. The low temperature decrease in the $\chi_M T$ value of all the three complexes is likely due to multiple factors such as magnetic anisotropy, intra- and inter-molecular antiferromagnetic exchange interactions and intermolecular dipolar exchange interactions.

Isothermal magnetization was performed on the polycrystalline sample of complexes 1–3 at 2.0 K (Fig. 3B). Upon increasing the magnetic field, the magnetic moment sharply increases in all three complexes (1–3) and the magnetic moment of complexes 1–3 tends to saturate around 27.12, 25.14 and 19.76$N\mu_B$, respectively, at 70 kOe. For complex 1, the saturation value is slightly lower than the expected saturation value (28$N\mu_B$). Modelling the magnetic data of anisotropic metal complexes in 2 and 3 is complicated by the first order orbital angular momentum and the spin–orbit coupling effect. However, 1 serves as a surrogate marker to better understand the nature of coupling between the lanthanide ions (in 2 and 3), if not quantitatively, at least qualitatively, as the electronic configuration of Gd(III) does not possess the orbital angular momentum. Based on the crystal structure and cautious about the over-parameterization, we have employed only one J to model the magnetic data of 1. This J represents the exchange interaction between the nearest neighbour in 1 (see the inset of Fig. 3A). In order to extract the spin Hamiltonian parameters for 1, we employed the following Heisenberg Dirac Van-Vleck (HDVV) Hamiltonian, and the magnetic susceptibility data were fitted by matrix diagonalization using PHI software.[17]

$$H = -2J_1(S_{Gd_1}\cdot S_{Gd_{1a}} + S_{Gd_1}\cdot S_{Gd_2} + S_{Gd_1}\cdot S_{Gd_{2a}} + S_{Gd_{1a}}\cdot S_{Gd_2} + S_{Gd_{1a}}\cdot S_{Gd_{2a}} + S_{Gd_2}\cdot S_{Gd_{2a}}) + g\mu_B H\cdot S$$

The data of 1 are very well reproduced with the following paramters, J_1 = −0.055 cm^{-1} and g = 2.01 and the parameters extracted from fitting are consistent with the other literature reports.[18] Significantly, a small J_1 value is likely due to the large intramolecular distance between the two Gd(III) with buried valence 4f orbitals. The parameters extracted from the $\chi_M T$ data fit are used to simulate the magnetization data of 1. The simulated data are in good agreement with the experimental data which exemplifies the reliability of the parameters extracted by modeling the magnetic data of 1.

In contrast to 2 and 3, the saturation value is significantly lower than the expected value (40$N\mu_B$ for 2 and 3). This is in line with the literature precedents and is due to the presence of anisotropy associated with complexes 2 and 3. It is further supported by the non-super imposable nature of reduced magnetization curves (Fig. S5 and S6 of the ESI†).

The $\chi_M T$ product for the Ln_2 complexes (Ln = Gd (4), Dy (5) and Ho (6).) at 300 K has values of 17.41, 28.62, and 27.65 cm^3 K mol^{-1}, respectively (Fig. 4A). These values are in excellent agreement with the expected values for two non-interacting

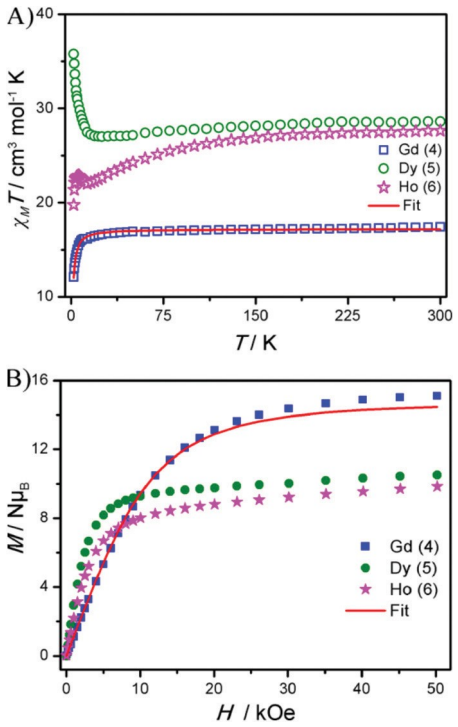

Fig. 4 (A) Temperature dependence of the product of magnetic susceptibility and temperature ($\chi_M T$) for 4–6 measured in the presence of 1 kOe. (B) Field dependence of magnetization for 4–6. The red solid line represents the best fit obtained for the experimental magnetic data of 4 using the parameters described in the main text.

lanthanide ions 7.9 cm^3 K mol^{-1} for one uncoupled Gd(III) ion ($^8S_{7/2}$, $S = 7/2$, $L = 0$, $g = 2.0$); 14.16 cm^3 K mol^{-1} for an uncoupled Dy(III) ion ($^6H_{15/2}$, $S = 5/2$, $L = 5$, $J = 15/2$ and $g_J = 4/3$); 14 cm^3 K mol^{-1} and the expected value for one isolated Ho(III) ion ($^5I_8$, $S = 2$, $L = 6$, $J = 8$ and $g_J = 5/4$) (see also Table 2). As the temperature decreases, the $\chi_M T$ product for 4 remains constant until a sharp decrease is observed below 10 K. This phenomenon indicates that the simple paramagnetic nature is witnessed in 4 from 300 K to 10 K and the observed $\chi_M T$ product is the sum of two isolated Gd(III) ions. By employing the HDVV Hamiltonian, the experimental magnetic data of both $\chi_M T(T)$ and $M(H)$ were fitted simultaneously. Excellent agreement between the fit and experimental magnetic data was observed using the parameters $J = -0.048$ cm^{-1} and $g = 1.99$. The data clearly indicate the presence of weak antiferromagnetic exchange interactions and the extracted parameters are consistent with the other reported complexes.[19] For 5 and 6 as the temperature decreases, the $\chi_M T$ product slightly decreases as expected due to the depopulation of the m_j sublevels of the ground J state. Below 25 K, the $\chi_M T$ product slightly rises for 6 indicating the onset of weak ferromagnetic coupling between the two Ho(III) ions. For 5, the increase of $\chi_M T$ product below 25 K is more pronounced indicating stronger ferromagnetic coupling between the two Dy(III) ions. The rapid rise observed for magnetization at 2 K for both 5 and 6 as a function of field confirms the population of a non-zero ground state.

The field dependent magnetization measurement performed for complexes 4–6 is shown in Fig. 4B at 2 K. It shows clearly that upon increasing the magnetic field, the magnetic moment sharply increases in all three complexes (4–6) and the magnetic moment of complexes 4–6 tends to saturate at 50 kOe. For complex 4, the value of the magnetic moment at 2.0 K is close to the expected value for an isotropic metal complex. While for complexes 5 and 6, the saturation value is significantly lower than the expected value.

Ac magnetic susceptibility studies. In order to check the magnetization relaxation dynamics, ac measurements were performed on the polycrystalline sample of complexes 2 and 5 with an applied oscillating field of 3.5 Oe with and without an external magnetic field. Complex 2 evidently shows temperature dependent out-of-phase susceptibility (χ''_M) signals without any well-resolved maxima (Fig. S7 in the ESI†). This hampers in extracting the effective energy barrier for the magnetization reversal of orientation. Evidently, Fig. S7† shows that more than one relaxation process is operational. This could be likely due to the two distinct geometries (SAP and TDD) shown by the Dy(III) in the asymmetric unit of 2. However, it is reported in the literature that even mononuclear Dy(III) complexes such as $[ZnDy(L^-)_2]^{3+}$ and [Dy(DOTA)] show more than one relaxation process such as Raman and Direct, apart from the Orbach process.[20] To understand the origin of the slow relaxation of magnetization, one of the Dy(III) ions that are crystallographically different in the unit cell of 2 needs to be replaced with a diamagnetic lanthanide ion such as La(III) or Lu(III) or Y(III). Unfortunately however, all the attempts to isolate such isostructural complexes of 2 were unsuccessful. The absence of well-resolve maxima in the χ''_M signal is likely due to the magnetization relaxation through the ground state m_j levels itself. Often, the fast quantum tunneling of magnetization (QTM) is suppressed by applying the external bias magnetic field. To find out the optimum external magnetic field, we performed isothermal field sweep ac measurements (Fig. S8 of the ESI†). Frequency dependent ac measurements at the optimum external magnetic field of 500 Oe were performed for 2 as shown in Fig. 5. It evidently shows that the frequency dependent out-of-phase susceptibility signals imply the slow relaxation of magnetization phenomenon associated with the complex. The χ''_M signals in Fig. 5B reveal that there are more than one relaxation process, which is firmly supported by the Cole–Cole plot of complex 2 (Fig. 6A). All attempts failed to fit the Cole–Cole plot of 2 with two relaxation processes and hence the major relaxation observed in the Cole–Cole plot data of 2 was fitted by considering a single relaxation process using the generalized Debye model equation given below.

$$\chi_{AC}(\omega) = \chi_S + \frac{\chi_T - \chi_S}{1 + (i\omega\tau)^{1-\alpha}} \quad (1)$$

In the above equation, α, ω, χ_S, χ_T, and τ represent the exponent parameter (which takes the value between 0 and 1), angular frequency, adiabatic magnetic susceptibility, isothermal magnetic susceptibility and relaxation time, respectively.

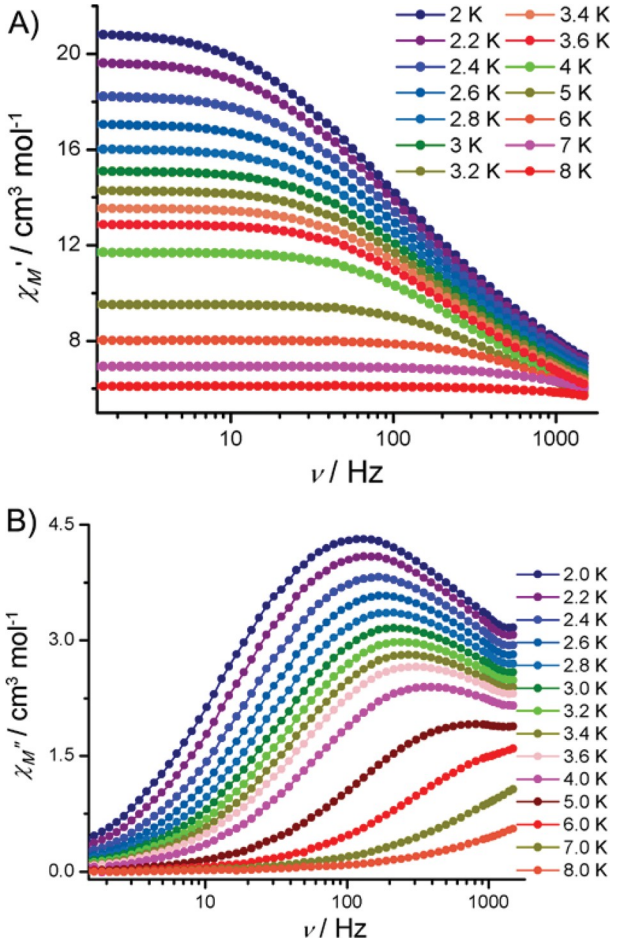

Fig. 5 Alternating current magnetic susceptibility measurement performed on the polycrystalline sample of 2 showing the frequency dependent in-phase ((χ'M, *top* panel A) and out-of-phase susceptibility signals (χ''M, *bottom* panel B) in the presence of an optimum external magnetic field of 0.05 kOe.

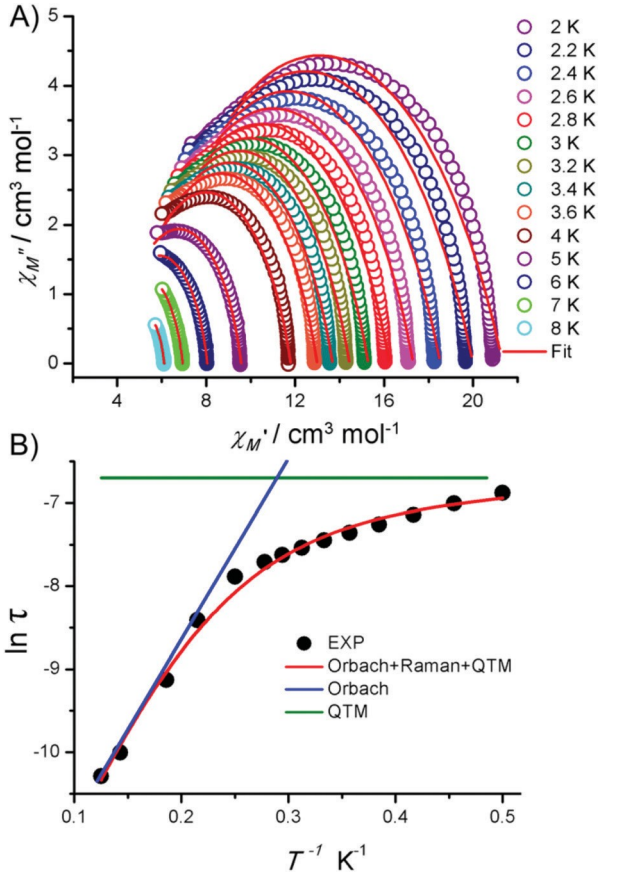

Fig. 6 Cole–Cole plot (panel A) and Arrhenius plot (panel B) of complex 2 are shown above. The solid red line in both panels denotes the best fit obtained for the parameters described in the main text.

The parameters extracted through the Cole–Cole fit of the experimental data are given in Table S4 of the ESI.† The α-values range from 0.18 to 0.37 which signifies the narrow distribution of the relaxation time in 2. The relaxation time extracted from the Cole–Cole data fit was utilized to construct an Arrhenius plot to estimate the barrier for the magnetization reversal (Fig. 6). The Arrhenius plot deviates from linearity below 2.5 K, suggesting that apart from the thermally assisted Orbach process, other relaxation mechanisms such as Raman, direct and QTM appear to be operative to change the magnetization direction. The Arrhenius plot in the entire temperature range was fitted by considering multiple relaxation processes using eqn (2) given below.

$$\frac{1}{\tau} = \frac{1}{\tau_{QTM}} + CT^{n} + \tau_0^{-1}\exp\left(\frac{-U_{eff}}{K_B T}\right) \quad (2)$$

In eqn (2), the first term on the right hand side of the equation corresponds to the QTM, while the second term denotes the Raman process and the final term represents the thermally assisted Orbach process. The fitted data are in reasonably good agreement with the experimental data using the parameters Orbach (U_{eff} = 18.07 cm^{-1}, τ_0 = 2.5 × 10^{-5} s), Raman (C = 0.78 s^{-1} K^{-3} and n = 3) and QTM (τ_{QTM} = 0.0012 s) (Fig. 6B).

In contrast to 2, ac susceptibility measurements performed on 5 show frequency dependent out-of-phase ac signals at zero applied magnetic field (Fig. 7). In Fig. 7B, the shifting of χ''M signals to a lower frequency upon decreasing the temperature is the classic signature of a molecule behaving as a single molecule magnet. Fig. 7B evidently suggests that there is only one single relaxation process which is consistent with the Cole–Cole data obtained for this complex.

The Cole–Cole plot was fitted considering a single relaxation using the generalized Debye equation (eqn (1)) and the parameters extracted through fitting are compiled in Table S5.† Exploiting the τ-values extracted from the Cole–Cole fit of the experimental data, an Arrhenius plot was constructed (Fig. 8B). As observed in 2, the Arrhenius plot of 5 exhibits a non-linear trend which implies that other relaxation mechanisms such as Raman, QTM or direct processes are operative apart from the Orbach process. The non-linear curve was fitted in the entire temperature range using eqn (2). The excellent fit

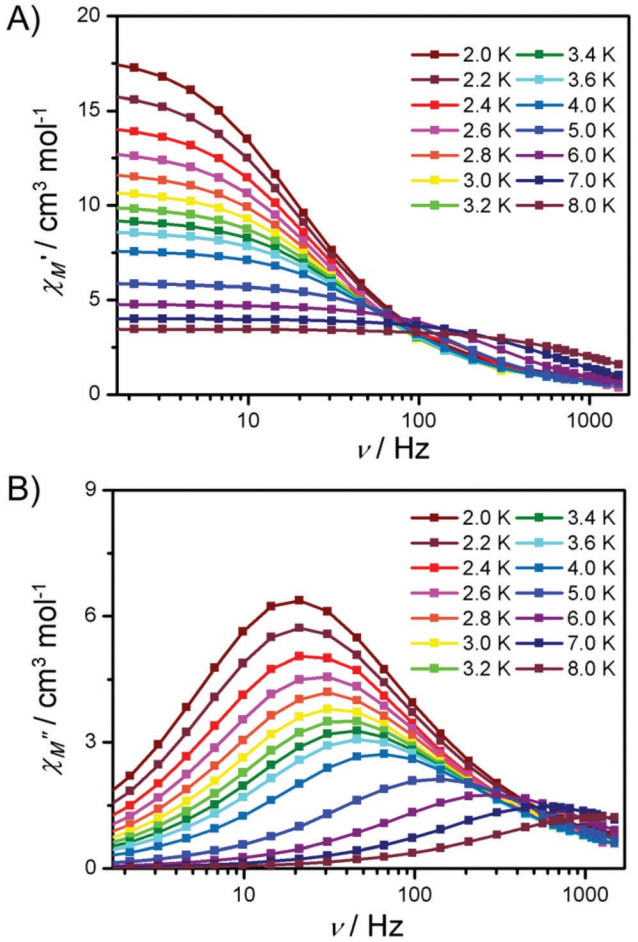

Fig. 7 Alternating current magnetic susceptibility measurement performed on the polycrystalline sample of 5 showing the frequency dependent in-phase (χ'_M, panel A) and out-of-phase susceptibility signals (χ''_M, panel B) in the absence of a bias field.

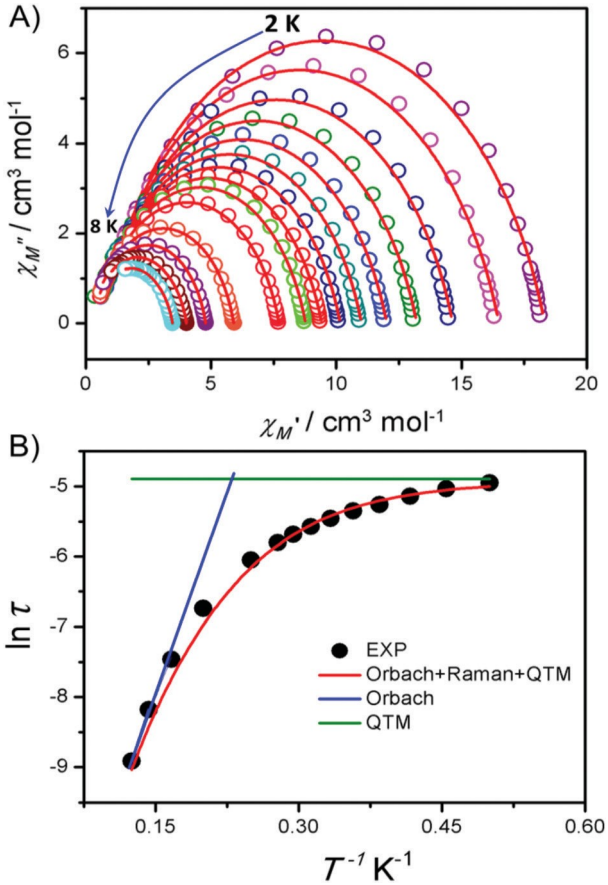

Fig. 8 Cole–Cole plot (panel A) and Arrhenius plot (panel B) of complex 5 are shown above. The solid red line in both panels denotes the best fit obtained for the parameters described in the main text.

of the data was obtained using the parameters Orbach (U_{eff} = 38.17 cm^{-1}, $\tau_0 = 1.85 \times 10^{-6}$ s), Raman ($C = 0.65\ s^{-1}\ K^{-4.5}$ and $n = 4.5$) and QTM ($\tau_{QTM} = 0.0075\ s^{-1}$) (Fig. 8B). The extracted effective energy barrier of 38.17 cm^{-1} is comparable to the other Dy(III) lanthanide dimers reported in the literature.[21]

To ascertain that the observed slow relaxation of magnetization is due to the collective behavior of the dimer or the molecular origin (considering the negligible exchange interaction between the two Dy(III) ions in 5), we attempted to replace one of the Dy(III) ions with a diamagnetic ion; unfortunately, we could not succeed in isolating the target complex, despite several attempts. This is likely due to the fact that one Dy(III) ion in 5 is related by the inversion center to other. Hence, 100% replacement of one Dy(III) by a diamagnetic center exclusively is a chemically challenging task.

The square antiprism geometry around the Dy(III) ions in both 2 and 5 is observed, however, the absence of zero field SMM behavior in 2 compared to 5 is quite surprising. To understand the relaxation dynamics in these complexes, the crystal structures of 2 and 5 were analyzed more carefully.

Although the Dy(III) ions exist in the SAP geometry in both 2 and 5, the extent of deviation (distortion) from the ideal square antiprism geometry around Dy(III) in 2 is larger (CShM value is 1.474) than in 5 (CShM value is 0.745). Furthermore, it is witnessed from the crystal structure that there is another crystallographically distinct molecule in 2 resulting in further reduction in the geometry around Dy(III) ions [*i.e.* triangular dodecahedron geometry (TDD)]. Likely, the combination of weak intramolecular exchange interactions, distortion from the ideal square antiprism geometry and dipolar interactions in 2 lead to a significant transverse component which is likely to trigger fast relaxation such as QTM in 2. This is firmly supported by the experimental fact that frequency dependent out-of-phase susceptibility signals were absent with well resolved maxima in the absence of an external magnetic field. The effect of the coordination geometry is well exemplified in some of the recent literature reports.[22]

As pointed out earlier, the two crystallographically distinct Dy(III) ions in the asymmetric unit of 2 possess different geometries (square anti-prism and TDD geometry). To understand the influence of geometry on the g_z orientation of these Dy(III) ions (assuming m_j of ±15/2 Krammers state stabilized) in 2, the electrostatic model developed by Chilton and Soncini was

employed.[23] Although there is a slight deviation in the g_z orientation predicted from more accurate *ab initio* calculations, the deviation in g_z calculated by the electrostatic model compared to the *ab initio* predicted orientation occurs marginally which is very well exemplified in the literature.[24] The g_z orientation predicted for all the Dy(III) ions in two crystallographically distinct units present in the crystal lattice of 2 using the electrostatic model is presented in Fig. 9.

The g_z orientation of Dy(III) where all the ions exist in the SAP geometry in one molecule (Dy1, Dy2 sites and its symmetrically equivalent) and the TDD geometry (Dy3, Dy4 sites and its symmetrically equivalent) in the second molecule of 2 is given in Fig. 9A and B, respectively. From Fig. 9A, it is noted that the ground state Krammers g_z orientation of the Dy2 ion deviates by 72° from the g_z orientation of the Dy1 ion. Furthermore, it is also observed that the g_z orientation of Dy1 (Dy2) deviates from its symmetrically related atom Dy1A (Dy2A) by 48.5° (45.4°). For the second asymmetric unit (ASU), the g_z orientation of the Dy3 site deviates from the Dy4 site by 65.9°, while the g_z orientation of the symmetrically related atoms Dy3–Dy3A and Dy4–Dy4A deviates by 38.5° and 34.9°, respectively.

To understand further the role of distortion and the g_z orientation of Dy(III) ions in 2, the g_z orientation of a Dy4 cubane complex with the molecular formula $[Ln_4(L)_4(Piv)_4]$ (7, Fig. 9c) reported elsewhere by Chandrasekhar and co-workers was compared. The rationale for choosing the latter complex is that this is the complex $[Ln_4(L)_4(Piv)_4]$ found to act as a zero field single molecule magnet with the largest barrier reported to date among the other cubane structures reported in the literature and it is somewhat structurally similar to the crystal structure of 2. Using the electrostatic model, the g_z orientation for all the four Dy(III) ions in 7 was computed and it is shown in Fig. 9C. Fig. 9C clarifies that the g_z orientations of all the Dy(III) ions are in the same direction which are near collinear to each other (the average g_z deviation observed is 3–5°). This suggests that the random orientation of the g_z axis in 2 reduces the overall magnetic anisotropy resulting in faster relaxation in 2 compared to 7. The non-collinear orientation of the g_z axis of each Dy(III) center in 2 is likely to trigger the magnetization relaxation *via* the under-barrier mechanism in the ground state itself rather than the thermally assisted Orbach process.

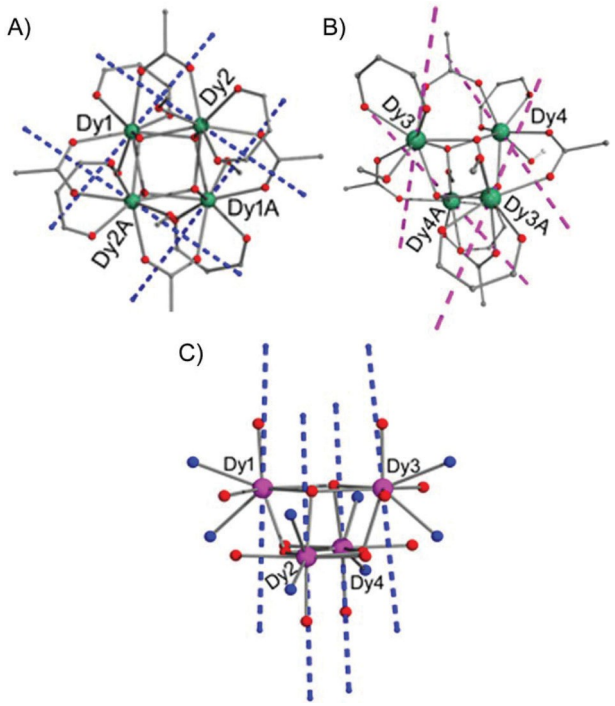

Fig. 9 The g_z orientation observed in the Dy(III) ion of two crystallographically distinct molecules (panels A and B) in the crystal lattice of 2. (C) The g_z orientation of a cubane structure (complex 7) with the largest U_{eff} reported to date among this cubane family is shown above for comparison.

In contrast, the signature of the QTM is less prominent in 5 compared to 2 (Fig. 7B). Moreover, the g_z orientations of the ground state (±15/2) Kramers doublet of Dy(III) ions in 5 are collinear with each other (Fig. 10).

The g_z anisotropic axes of both the Dy(III) ions orient towards the Dy···Dy axis, which does not pass through the Dy···Dy axis. A favorable ligand field around Dy(III) ions and the collinear arrangement of the easy axis (g_z) on both the Dy(III) ions along with the presence of ferromagnetic exchange interactions between the Dy(III) ions in 5 favor the magnetization vector relaxation *via* other excited Krammers doublets resulting in thermally assisted slow relaxation of magnetization (Orbach process) predominantly (Fig. 7).[25]

Estimation of MCE. In order to understand the MCE of the isotropic metal complexes 1 and 4, detailed isothermal field dependent magnetization measurements were performed on the polycrystalline samples from 2.0 to 15 K. The change in magnetic entropy ($-\Delta S_m$) and the change in adiabatic temperature (ΔT_{ad}) are the two salient thermodynamic parameters of the magneto-caloric effect (MCE). Using the Maxwell's thermodynamic relation and from the detailed magnetization

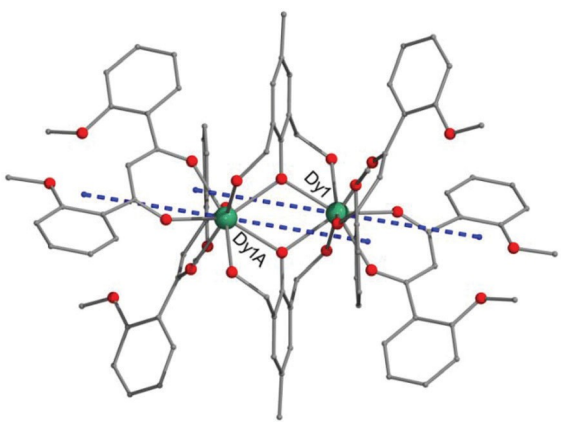

Fig. 10 The g_z orientation observed in the Dy(III) ions in complex 5 computed using the electrostatic model.

measurements of complexes, the change in the magnetic entropy observed for these complexes was estimated.

$$-\Delta S_m(T; H) = \int_{H_i}^{H_f} \left[\frac{\partial M(T; H)}{\partial T}\right]_H dH \quad (3)$$

where H_i and H_f are the initial and final applied magnetic field, respectively.

The $-\Delta S_m$ value of 25.57 J kg^{-1} K^{-1} at 3.0 K for ΔH = (0–70 k Oe, Fig. 11) for 1 is extracted from the magnetization measurement. The extracted $-\Delta S_m$ value is comparable to other related structures reported in the literature.[18a] However, the observed $-\Delta S_m$ value for 1 is relatively low compared to a coordination polymeric chain of the tetrameric Gd(III) complex.[26] This is due to the less mass density ratio observed in 1 compared to the polymeric chain. In fact the importance of the mass density ratio to reveal a better magnetic coolant material was elegantly reported by Evangelisti and co-workers and others recently.[27] Theoretically, the calculated full magnetic entropy content of $R\ln(8)$ = 17.3 J mol^{-1} K^{-1} = 29.28 J kg^{-1} K^{-1} per mole of Gd(III) is involved, as it is expected from $R\ln(2S+1)$ and $S = 7/2$ (where R is the universal gas constant).

Similar to 1, in complex 4, the change in the magnetic entropy is estimated using Maxwell's equation mentioned above with the value of 12.93 J kg^{-1} K^{-1} (Fig. 11D). This value is slightly lower than the theoretically expected value of 16.71 J kg^{-1} K^{-1} [$R\ln(8)$ and $S = 7/2$]. This is likely due to the presence of the exchange interaction between the molecules which lifts the degeneracy of the other energy level which prevents the easy polarization of the spin. Also, even in isotropic metal complexes like 1 and 4, magnetic anisotropy originated due to the ligand field around the Gd(III).[28] The existence of magnetic anisotropy does not allow the easy polarization of spin orientation resulting in reduced magnetic coolant efficiency. The observed $-\Delta S_m$ value is comparable to the other related structures and some of the isotropic 3d–4f clusters reported in the literature.[29] However, for both complexes (1 and 4), the observed $-\Delta S_m$ value is lower than the acetate bridged Gd(III) dimer,[27b] Co–Gd grid complexes reported by Winpenny and co-workers and extended three dimensional GdF_3 complexes.[30] magnetic field from 2–15 K temperature range.

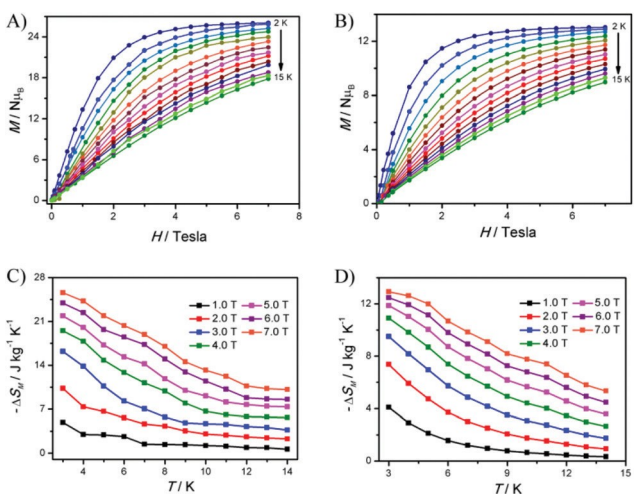

Fig. 11 Detailed isothermal field dependant magnetization measurement performed on the polycrystalline sample of 1 (A) and 4 (B) measured from 0–7 Tesla at the indicated temperatures. The magnetic entropy change ($-\Delta S_m$) for the complex 1 (C) and 4 (D) in the indicated

As pointed out earlier, the magnetic entropy is directly pro- portional to the overall spin ground state associated with the cluster. However, there are clusters with a large ground state registered with a low $-\Delta S_m$ value[31] compared to the complexes 1 and 4 emphasizing the importance of the mass density ratio.

Experimental

General information and instrumentation

The general reagents are analytical grade and used as received without further purification. LH was prepared according to the literature procedure.[32] Hydrated lanthanum trihalides were prepared from the corresponding oxides by neutralizing with concentrated HCl, followed by evaporation to dryness. Triethylamine, pivH, LH'_3 and common organic solvents were purchased from commercial sources and used without further purification. Infrared spectra were recorded on a JASCO-5300 FT-IR spectrometer using KBr pellets. Thermogravimetric ana- lyses were carried out on an SDT-Q600 supplied by Ta instru- ments. Elemental analysis was performed on a flash EA series 1112 CHNS analyzer. Magnetic measurements were carried out in the Department of Chemistry (IIT Bombay) and Unitat de Mesures Magnètiques (Universitat de Barcelona) on polycrys- talline samples (*approximately* 30 mg) with a Quantum Design SQUID MPMS-XL magnetometer equipped with a 7 T magnet. Diamagnetic corrections were calculated using Pascal's con- stants and an experimental correction for the sample holder was applied. Single crystal X-ray diffraction data for all the compounds were collected on a Bruker Smart Apex CCD area detector system (λ (Mo Kα) = 0.71073 Å) at 100(2) K. Data pro- cessing was accomplished by using SAINT PLUS and the struc- tures were solved by using SHELXS-97 and refined using the SHELXL-2014/7 program.[33] All non-hydrogen atoms were refined anisotropically by full matrix least-squares cycles on F^2. Hydrogen atoms were introduced at calculated positions and refined as a riding model. Crystal data parameters for com- plexes 1–6 are summarized in Table 1.

General synthetic procedure for compounds 1–6

To a methanolic solution of ligand LH and pivH, $LnCl_3 \cdot 6H_2O$ was added and stirred at room temperature for 10 minutes. To this solution, triethylamine was added dropwise and the mixture was stirred for further 12 h at room temperature resulting in a pale yellow precipitate which was washed with methanol, dried and re-dissolved in CH_3CN/MeOH for crystal- lization. Pale yellow block shaped crystals suitable for X-ray crystallography were obtained by slow evaporation of the solvent mixture under aerobic conditions. The same procedure was followed for the synthesis of 4, 5 and 6, where LH_3 was

used instead of pivH. Crystals suitable for X-ray analysis were obtained by slow evaporation of the solvent mixture DMF/MeOH.

Compound 1. LH (0.150 g, 0.527 mmol), PivH (0.053 g, 0.527 mmol), $GdCl_3 \cdot 6H_2O$ (0.196 g, 0.527 mmol), Et_3N (0.29 mL, 2.108 mmol). Yield: 0.450 g, 61.14% (based on Gd). Mp: 162 °C (dec). IR (KBr) cm^{-1}: 3599(b), 3073(w), 2959(s), 2865(w), 2832(m), 1610(w), 1561(m), 1506(m), 1478(s), 1396(m), 1308(s), 1237(s), 1177(m), 1023(s), 947(m), 892(m), 760(s). Anal. calcd (%) for $C_{92}H_{116}O_{32}Gd_4$ (2362.85): C, 46.76; H, 4.94. Found: C, 46.45; H, 4.85.

Compound 2. LH (0.150 g, 0.527 mmol), PivH (0.053 g, 0.527 mmol), $DyCl_3 \cdot 6H_2O$ (0.198 g, 0.527 mmol), Et_3N (0.29 mL, 2.108 mmol). Yield: 0.450 g, 60.60% (based on Dy). Mp: 164 °C (dec). IR (KBr) cm^{-1}: 3583(b), 3073(w), 2953(s), 2865(w), 2837(m), 1604(w), 1544(m), 1511(m), 1478(s), 1391(m), 1308(s), 1237(s), 1182(m), 1018(s), 936(m), 821(m), 749(s). Anal. calcd (%) for $C_{92}H_{116}O_{32}Dy_4$ (2369.53): C, 46.35; H, 4.90. Found: C, 46.27; H, 4.85.

Compound 3. LH (0.150 g, 0.527 mmol), PivH (0.053 g, 0.527 mmol), $HoCl_3 \cdot 6H_2O$ (0.200 g, 0.527 mmol), Et_3N (0.29 mL, 2.108 mmol). Yield: 0.320 g, 62.75% (based on Ho). Mp: 164 °C (dec). IR (KBr) cm^{-1}: 3583(b), 3073(w), 2953(s), 2865(w), 2832(m), 1599(w), 1550(m), 1506(m), 1478(s), 1396(m), 1308(s), 1232(s), 1182(m), 1018(s), 941(m), 821(m), 755(s). Anal. calcd (%) for $C_{92}H_{116}O_{32}Ho_4$ (2393.56): C, 46.16; H, 4.88. Found: C, 46.05; H, 4.85.

Compound 4. LH (0.1 g, 0.369 mmol), LH′$_3$ (0.062 g, 0.369 mmol), $GdCl_3 \cdot 6H_2O$ (0.137 g, 0.369 mmol), Et_3N (0.20 mL, 1.476 mmol). Yield: 0.256 g, 60% (based on Gd). Mp: 162 °C (dec). IR (KBr) cm^{-1}: 3599(b), 3075(w), 2995(s), 2840(w), 1668(s), 1609(s), 1561(s), 1515(m), 1486(s), 1396(m), 1237(s), 1177(m), 1023(s), 947(m), 892(m), 760(s). Anal. calcd (%) for $C_{98}H_{106}N_4O_{26}Gd_2$(2070.36): C, 58.12; H, 4.67. Found: C, 58.05; H, 4.85.

Compound 5. LH (0.1 g, 0.369 mmpl), LH′$_3$ (0.062 g, 0.369 mmol), $DyCl_3 \cdot 6H_2O$ (0.139 g, 0.369 mmol), Et_3N (0.20 mL, 1.476 mmol). Yield: 0.286 g, 64% (based on Dy). Mp: 173 °C (dec). IR (KBr) cm^{-1}: 3600(b), 3073(w), 2997(s), 2838(w), 1665(s), 1605(s), 1550(s), 1512(m), 1484(s), 1380(m), 1243(s), 1161(m), 1019(s), 945(m), 895(m), 750(s). Anal. calcd (%) for $C_{98}H_{106}N_4O_{26}Dy_2$(2080.86): C, 56.56; H, 5.13. Found: C, 56.05; H, 5.15.

Compound 6. LH (0.1 g, 0.369 mmpl), LH′$_3$ (0.062 g, 0.369 mmol), $HoCl_3 \cdot 6H_2O$ (0.140 g, 0.369 mmol), Et_3N (0.20 mL, 1.476 mmol). Yield: 0.290 g, 65% (based on Ho). Mp: 164 °C (dec). IR (KBr) cm^{-1}: 3597(b), 3068(w), 2925(s), 2838(w), 1660(s), 1609(s), 1594(s), 1506(m), 1479(s), 1391(m), 1249(s), 1161(m), 1013(s), 949(m), 898(m), 756(s). Anal. calcd (%) for $C_{98}H_{106}N_4O_{26}Ho_2$ (2085.72): C, 56.43; H, 5.12. Found: C, 56.05; H, 5.15.

Conclusions

A family of tetranuclear and dinuclear lanthanide complexes were isolated and structurally characterized by single crystal X-ray diffraction. Magnetic susceptibility measurements were performed on the polycrystalline sample of 1–6. Detailed investigation on the magnetization relaxation dynamics was performed on complex 2 which reveals that the g_z-axis is randomly oriented in both the crystallographically distinct molecules within the crystal lattice of 2. This combined with large distortion around Dy(III) ions triggers faster relaxation. Due to this, only field induced slow relaxation of magnetization behavior was witnessed. On the other hand, complex 5 shows zero field χ''_M signals with an effective energy barrier of 38.71 K and an pre-exponential factor (τ_0) = 1.85 × 10^{-6} s. The distinct magnetization relaxation behavior in 5 (compared to 2) is correlated with the suitable ligand field and the ideal square antiprism geometry around Dy(III), the collinear arrangement of g_z orientation and the ferromagnetic exchange coupling in 5 quenching the under barrier mechanism to some extent facilitate the Orbach process. The studies presented here clearly emphasize the influence of the ligand field on the magnetization relaxation dynamics while the isotropic metal complexes 1 and 4 show the change in the magnetic entropy ($-\Delta S_m$) of = 25.57 and 12.93 J kg^{-1} K^{-1}, respectively. This study reiterates the fact that the magnetic density is a crucial factor to increase the $-\Delta S_m$ value to design better magnetic refrigerants.

Conflicts of interest

There are no conflicts to declare.

Acknowledgements

V. B. thanks DST-SERB, India and UPE Phase II for financial support. A. R. thanks UGC for the fellowship. M. S. thanks DST -SERB INSA, IIT Bombay for financial support. ECS thanks Spanish Government (Grant CTQ2012-32247) for financial support.

References

1 (*a*) D. N. Woodruff, R. E. P. Winpenny and R. A. Layfield, *Chem. Rev.*, 2013, 113, 5110–5148; (*b*) S. M. Neville, G. J. Halder, K. W. Chapman, M. B. Duriska, B. Moubaraki, K. S. Murray and C. J. Kepert, *J. Am. Chem. Soc.*, 2009, 131, 12106–12108; (*c*) L. Ungur, S. K. Langley, T. N. Hooper, B. Moubaraki, E. K. Brechin, K. S. Murray and L. F. Chibotaru, *J. Am. Chem. Soc.*, 2012, 134, 18554–18557; (d) J. J. Le Roy, L. Ungur, L. Korobkov, L. F. Chibotaru and M. Murugesu, *J. Am. Chem. Soc.*, 2014, 136, 8003–8010; (e) N. F. Chilton, D. Collison, E. J. L. McInnes, R. E. P. Winpenny and A. Soncini, *Nat. Commun.*, 2013, 4, 2551–2553; (*f*) V. Chandrasekhar, A. Dey, S. Das, M. Rouzières and R. Clérac, *Inorg. Chem.*, 2013, 52, 2588–2598; (*g*) J. Goura, J. P. S. Walsh, F. Tuna and V. Chandrasekhar, *Inorg. Chem.*, 2014, 53, 3385–3391; (*h*) A. Baniodeh, V. Mereacre, N. Magnani, Y. Lan,

J. A. Wolny, V. Schünemann, C. E. Anson and A. K. Powell, *Chem. Commun.*, 2013, 49, 9666–9668; (*i*) A. Baniodeh, N. Magnani, S. Bräse, C. E. Anson and A. K. Powell, *Dalton Trans.*, 2015, 44, 6343–6347; (*j*) B. Hussain, D. Savard, T. J. Burchell, W. Wernsdorfer and M. Murugesu, *Chem. Commun.*, 2009, 1100–1102; (*k*) R. J. Blagg, L. Ungur, F. Tuna, J. Speak, P. Comar, D. Collison, W. Wernsdorfer, E. J. L. McInnes, L. F. Chibotaru and R. E. P. Winpenny, *Nat. Chem.*, 2013, 5, 673–678; (*l*) C. A. P. Goodwin, F. Ortu, D. Reta, N. F. Chilton and D. P. Mills, *Nature*, 2017, 548, 439–442; (*m*) F.-S. Guo, B. M. Day, Y.-C. Chen, M.-L. Tong, A. Mansikkamaeki and R. A. Layfield, *Angew. Chem., Int. Ed.*, 2017, 56, 11445–11449; (*n*) L. Ungur, S.-Y. Lin, J. Tang and L. F. Chibotaru, *Chem. Soc. Rev.*, 2014, 43, 6894–6905 and references therein. (*o*) C. Das, S. Vaidya, T. Gupta, J. M. Frost, M. Righi, E. K. Brechin, M. Affronte, G. Rajaraman and M. Shanmugam, *Chem. – Eur. J.*, 2015, 44, 15639–15650; (*p*) K. R. Vignesh, A. Soncini, S. K. Langley, W. Wernsdorfer, K. S. Murray and G. Rajaraman, *Nat. Commun.*, 2017, 8, 1023.

2 (*a*) M. Evangelisti and E. K. Brechin, *Dalton Trans.*, 2010, 39, 4672–4676; (*b*) J. W. Sharples and D. Collison, *Polyhedron*, 2013, 54, 91–103; (*c*) R. Sessoli, *Angew. Chem., Int. Ed.*, 2012, 51, 43–45, (*Angew. Chem.*, 2012, 124, 43–45); (d) E. Cremades, S. Gûmez-Coca, D. Aravena, S. Alvarez and E. Ruiz, *J. Am. Chem. Soc.*, 2012, 134, 10532–10542; (e) G. Lorusso, M. A. Palacios, G. S. Nichol, E. K. Brechin, O. Roubeau and M. Evangelisti, *Chem. Commun.*, 2012, 48, 7592–7594; (*f*) G. Lorusso, J. W. Sharples, E. Palacios, O. Roubeau, E. K. Brechin, R. Sessoli, A. Rossin, F. Tuna, E. J. L. McInnes, D. Collison and M. Evangelisti, *Adv. Mater.*, 2013, 25, 4653–4656.

3 (*a*) K. Katoh, R. Asano, A. Miura, Y. Horii, T. Morita, B. K. Breedlove and M. Yamashita, *Dalton Trans.*, 2014, 43, 7716–7725; (*b*) K. Suzuki, R. Sato and N. Mizuno, *Chem. Sci.*, 2013, 4, 596–600; (*c*) F. Yang, Q. Zhou, G. Zeng, G. Li, L. Gao, Z. Shi and S. Feng, *Dalton Trans.*, 2014, 43, 1238–1245; (*d*) P. Zhang, L. Zhang, S.-Y. Lin, S. Xue and J. Tang, *Inorg. Chem.*, 2013, 52, 4587–4592; (*e*) W.-B. Sun, B. Yan, L.-H. Jia, B.-W. Wang, Q. Yang, X. Cheng, H.-F. Li, P. Chen, Z.-M. Wang and S. Gao, *Dalton Trans.*, 2016, 45, 8790–8794; (*f*) J. R. Long, F. Habib, P.-H. Lin, I. Korobkov, G. Enright, L. Ungur, W. Wernsdorfer, L. Chibotaru and M. Murugesu, *J. Am. Chem. Soc.*, 2011, 133, 5319–5328; (*g*) R. A. Layfield, J. J. W. McDouall, S. A. Sulway, F. Tuna, D. Collison and R. E. P. Winpenny, *Chem. – Eur. J.*, 2010, 16, 4442–4446; (*h*) G.-F. Xu, Q.-L. Wang, P. Gamez, Y. Ma, R. Clerac, J. Tang, S.-P. Yan, P. Cheng and D.-Z. Liao, *Chem. Commun.*, 2010, 46, 1506–1508; (*i*) Y. Ma, G.-F. Xu, X. L. Yang, L.-C. Li, J. Tang, S.-P. Yan, P. Cheng and D.-Z. Liao, *Chem. Commun.*, 2009, 46, 8264–8266; (*j*) S. A. Sulway, R. A. Layfield, F. Tuna, W. Wernsdorfer and R. E. P. Winpenny, *Chem. Commun.*, 2012, 48, 1508– 1510; (*k*) P. H. Lin, W. B. Sun, M. F. Yu, G. M. Li, P. F. Yan and M. Murugesu, *Chem. Commun.*, 2011, 47, 10993– 10995; (*l*) Y. N. Guo, X. H. Chen, S. Xue and J. Tang, *Inorg. Chem.*, 2011, 50, 9705–9713; (*m*) Y.-N. Guo, G.-F. Xu, W. Wernsdorfer, L. Ungur, Y. Guo, J. Tang, H. J. Zhang, L. F. Chibotaru and A. K. Powell, *J. Am. Chem. Soc.*, 2011, 133, 11948–11951; (*n*) E. M. Fatila, M. Rouzières, M. C. Jennings, A. J. Lough, R. Clérac and K. E. Preuss, *J. Am. Chem. Soc.*, 2013, 135, 9596–9599; (*o*) K. Katoh, T. Kajiwara, M. Nakano, Y. Nakazawa, W. Wernsdorfer, N. Ishikawa, B. K. Breedlove and M. Yamashita, *Chem. – Eur. J.*, 2011, 17, 117–122.

4 (*a*) P. C. Andrews, G. B. Deacon, R. Frank, B. H. Fraser, P. C. Junk, J. G. MacLellan, M. Massi, B. Moubaraki, K. S. Murray and M. Silberstein, *Eur. J. Inorg. Chem.*, 2009, 744–751; (*b*) J. Tang, I. Hewitt, N. T. Madhu, G. Chastanet, W. Wernsdorfer, C. E. Anson, C. Benelli, R. Sessoli and A. K. Powell, *Angew. Chem., Int. Ed.*, 2006, 45, 1729–1733; (*c*) S. Xue, L. Zhao, Y.-N. Guo, P. Zhang and J. Tang, *Chem. Commun.*, 2012, 48, 8946–8948.

5 S.-Y. Lin and J. Tang, *Polyhedron*, 2014, 83, 185–196.

6 (*a*) R. J. Blagg, C. A. Muryn, E. J. L. McInnes, F. Tuna and R. E. P. Winpenny, *Angew. Chem., Int. Ed.*, 2011, 50, 6530–6533; (*b*) S. Das, S. Hossain, A. Dey, S. Biswas, J.-P. Sutter and V. Chandrasekhar, *Inorg. Chem.*, 2014, 53, 5020–5028; (*c*) S.-Y. Lin, W. Wernsdorfer, L. Ungur, A. K. Powell, Y.-N. Guo, J. Tang, L. Zhao, L. F. Chibotaru and H.-J. Zhang, *Angew. Chem., Int. Ed.*, 2012, 51, 12767– 12771; (*d*) J. W. Sharples, Y.-Z. Zheng, F. Tuna, E. J. L. McInnes and D. Collison, *Chem. Commun.*, 2011, 47, 7650–7652.

7 F. Habib, G. Brunet, V. Vieru, I. Korobkov, L. F. Chibotaru and M. Murugesu, *J. Am. Chem. Soc.*, 2013, 135, 13242–13245.

8 (*a*) K. Bernot, J. Luzon, L. Bogani, M. Etienne, C. Sangregorio, M. Shanmugam, A. Caneschi, R. Sessoli and D. Gatteschi, *J. Am. Chem. Soc.*, 2009, 131, 5573–5579; (*b*) S. D. Jiang, B. W. Wang, G. Su, Z. M. Wang and S. Gao, *Angew. Chem., Int. Ed.*, 2010, 49, 7448–7451; (*c*) D.-P. Li, T.-W. Wang, C.-H. S. Li, D.- Liu, Y.-Z. Li and X.-Z. You, *Chem. Commun.*, 2010, 46, 2929–2931; (*d*) Y. Ma, G.-F. Xu, X. Yang, L.-C. Li, J. Tang, S.-P. Yan, P. Cheng and D.-Z. Liao, *Chem. Commun.*, 2010, 46, 8264–8266.

9 G.-J. Chen, C.-Y. Gao, J.-L. Tian, J. Tang, W. Gu, X. Liu, S.-P. Yan, D.-Z. Liao and P. Cheng, *Dalton Trans.*, 2011, 40, 5579–5583.

10 Y. Bi, Y.-N. Guo, L. Zhao, Y. Guo, S.-Y. Lin, S. D. Jiang, J. Tang, B. W. Wang and S. Gao, *Chem. – Eur. J.*, 2011, 17, 12476–12481.

11 (*a*) V. Baskar and P. W. Roesky, *Z. Anorg. Allg. Chem.*, 2005, 631, 2782–2785; (*b*) M. T. Gamer, Y. Lan, P. W. Roesky, A. K. Powell and R. Clerac, *Inorg. Chem.*, 2008, 47, 6581–6583; (*c*) S. Datta, V. Baskar, H. Li and P. W. Roesky, *Eur. J. Inorg. Chem.*, 2007, 4216–4226; (*d*) M. Addamo, G. Bombieri, E. Foresti, M. D. Grillone and M. Volpe, *Inorg. Chem.*, 2004, 43, 1603–1605; (*e*) P. C. Andrews, T. Beck, C. M. Forsyth, B. H. Fraser, P. C. Junk, M. Massi and P. W. Roesky, *Dalton Trans.*, 2007, 5651–5654; (*f*) E. H. Barash, P. S. Coan, E. B. Lobkovsky, W. E. Streib

and K. G. Caulton, *Inorg. Chem.*, 1993, 32, 497–501; (*g*) R. Wang, D. Song and S. Wang, *Chem. Commun.*, 2002, 368–369; (*h*) Y. Wu, S. Morton, X. Kong, G. S. Nichol and Z. Zheng, *Dalton Trans.*, 2011, 40, 1041–1046; (*i*) M. Yadav, A. Mondal, V. Mereacre, S. K. Jana, A. K. Powell and P. W. Roesky, *Inorg. Chem.*, 2015, 54, 7846–7856; (*j*) Y.-C. Hui, Y.-S. Meng, Z. Li, Q. Chen, H.-L. Sun, Y.-Q. Zhangd and S. Gao, *CrystEngComm*, 2015, 17, 5620–5624; (*k*) D. T. Thielemann, A. T. Wagner, Y. Lan, P. Oña-Burgos, I. Fernãndez, E. S. Rösch, D. K. Kölmel, A. K. Powell, S. Bräse and P. W. Roesky, *Chem. – Eur. J.*, 2015, 21, 2813–2820.

12 (*a*) S. Tanase, M. Viciano-Chumillas, J. M. M. Smits, R. D. Gelder and J. Reedijk, *Polyhedron*, 2009, 28, 457–460; (*b*) E. W. Aniscough, A. M. Brodie, R. J. Cresswell and J. M. Waters, *Inorg. Chim. Acta*, 1998, 277, 37–45; (*c*) A. K. Jami, P. V. V. N. Kishore and V. Baskar, *Polyhedron*, 2009, 28, 2284–2286; (*d*) P. C. Andrews, T. Beck, B. H. Fraser, P. C. Junk, M. Massi, B. Moubaraki, K. S. Murry and M. Silberstein, *Polyhedron*, 2009, 28, 2123–2130.

13 (*a*) Y. L. Hou, G. Xiong, P. F. Shi, R. R. Cheng, J. Z. Cui and B. Zhao, *Chem. Commun.*, 2013, 49, 6066–6068; (*b*) P. F. Shi, Y. Z. Zheng, X. Q. Zhao, G. Xiong, B. Zhao, F. F. Wan and P. Cheng, *Chem. – Eur. J.*, 2012, 18, 15086–15091.

14 (*a*) Y. Z. Zheng, G. J. Zhou, Z. P. Zheng and R. E. P. Winpenny, *Chem. Soc. Rev.*, 2014, 43, 1462–1475; (*b*) M. Evangelisti and E. K. Brechin, *Dalton Trans.*, 2010, 39, 4672; (*c*) R. Sessoli, *Angew. Chem., Int. Ed.*, 2012, 51, 43–45.

15 (*a*) S. Alvarez, P. Alemany, D. Casanova, J. Cirera, M. Llunell and D. Avnir, *Coord. Chem. Rev.*, 2005, 249, 1693–1780; (*b*) D. Casanova, M. Llunell, P. Alemany and S. Alvarez, *Chem. – Eur. J.*, 2005, 11, 1479–1494.

16 (*a*) Y. J. Gao, G. F. Xu, L. Zhao, J. Tang and Z. L. Liu, *Inorg. Chem.*, 2009, 48, 11495–11497; (*b*) H. S. Ke, P. Gamez, L. Zhao, G. F. Xu, S. F. Xue and J. Tang, *Inorg. Chem.*, 2010, 49, 7549–7557; (*c*) C.-M. Liu, D.-Q. Zhang, X. Hao and D.-B. Zhu, *Cryst. Growth Des.*, 2012, 12, 2948–2954; (*d*) S. Das, A. Dey, S. Biswas, E. Colacio and V. Chandrasekhar, *Inorg. Chem.*, 2014, 53, 3417–3426; (*e*) Y. Li, J.-W. Yu, Z.-Y. Liu, E.-C. Yang and X.-J. Zhao, *Inorg. Chem.*, 2015, 54, 153–160; (*f*) D. Savard, P.-H. Lin, T. J. Burchell, I. Korobkov, W. Wernsdorfer, R. Clérac and M. Murugesu, *Inorg. Chem.*, 2009, 48, 11748–11754; (*g*) X.-J. Kong, L.-S. Long, L.-S. Zheng, R. Wang and Z. Zheng, *Inorg. Chem.*, 2009, 48, 3268–3273; (*h*) O. A. Gerasko, E. A. Mainicheva, M. I. Naumova, O. P. Yurjeva, A. Alberola, C. Vicent, R. Llusar and V. P. Fedin, *Eur. J. Inorg. Chem.*, 2008, 416–424; (*i*) B.-Q. Ma, D.-S. Zhang, S. Gao, T.-Z. Jin, C.-H. Yan and G.-X. Xu, *Angew. Chem., Int. Ed.*, 2000, 39, 3644–3646; (*j*) V. Baskar and P. W. Roesky, *Dalton Trans.*, 2006, 676–679; (*k*) Z. P. Zheng, *Chem. Commun.*, 2001, 2521–2529; (*l*) X. J. Kong, Y. L. Wu, L. S. Long, L. S. Zheng and Z. P. Zheng, *J. Am. Chem. Soc.*, 2009, 131, 6918–6919; (*m*) A. S. R. Chesman, D. R. Turner, B. Moubaraki, K. S. Murray, G. B. Deacon and S. R. Batten, *Dalton Trans.*, 2012, 41, 3751–3757.

17 N. F. Chilton, R. P. Anderson, L. D. Turner, A. Soncini and K. S. Murray, *J. Comput. Chem.*, 2013, 34, 1164–1175.

18 (*a*) C. Das, S. Vaidya, T. Gupta, J. M. Frost, M. Righi, E. K. Brechin, M. Affronte, G. Rajaraman and M. Shanmugam, *Chem. – Eur. J.*, 2015, 21, 15639–15650; (*b*) S. Y. Lin, X.-L. Li, H. Ke and Z. Xu, *CrystEngComm*, 2015, 17, 9167–9174.

19 G. Brunet, F. Habib, I. Korobkov and M. Murugesu, *Inorg. Chem.*, 2015, 54, 6195–6202; P. Comba, M. Großhauser, R. Klingeler, C. Koo, Y. Lan, D. Muller, J. Park, A. Powell, M. J. Riley and H. Wadepoh, *Inorg. Chem.*, 2015, 54, 11247–11258.

20 (*a*) A. Upadhyay, S. K. Singh, C. Das, R. Mondol, S. K. Langley, K. S. Murray, G. Rajaraman and M. Shanmugam, *Chem. Commun.*, 2014, 50, 8838–8841; (*b*) G. Cucinotta, M. Perfetti, J. Luzon, M. Etienne, P.-E. Car, A. Caneschi, G. Calvez, K. Bernot and R. Sessoli, *Angew. Chem., Int. Ed.*, 2012, 51, 1606–1610.

21 (*a*) Y.-L. Wang, C.-B. Han, Y.-Q. Zhang, Q.-Y. Liu, C.-M. Liu and S.-G. Yin, *Inorg. Chem.*, 2016, 55, 5578–5584; (*b*) N. J. Yutronkie, I. A. Kuhne, I. Korobkov, J. L. Brusso and M. Murugesu, *Chem. Commun.*, 2016, 52, 677; (*c*) Y.-S. Ding, T. Han, Y.-Q. Hu, M. Xu, S. Yang and Y.-Z. Zheng, *Inorg. Chem. Front.*, 2016, 3, 798–807; (*d*) S. Biswas, S. Das, G. Rogez and V. Chandrasekhar, *Eur. J. Inorg. Chem.*, 2016, 3322–3329; (*e*) P. Bag, C. K. Rastogi, S. Biswas, S. Sivakumar, V. Mereacre and V. Chandrasekhar, *Dalton Trans.*, 2015, 44, 4328–4340; (*f*) L.-F. Wang, J.-Z. Qiu, J.-Y. Hong, Y.-C. Chen, Q.-W. Li, J.-H. Jia, J. Jover, E. Ruiz, J.-L. Liu and M.-L. Tong, *Inorg. Chem.*, 2017, 56, 8829–8836.

22 (*a*) G. Cosquer, F. Pointillart, S. Golhen, O. Cador and L. Ouahab, *Chem. – Eur. J.*, 2013, 19, 7895–7903; (*b*) A. K. Mondal, S. Goswami and S. Konar, *Dalton Trans.*, 2015, 44, 5086–5094; (*c*) A. K. Mondal, S. Goswami and S. Konar, *Magnetochemistry*, 2016, 2, 35; (*d*) D. N. Woodruff, F. Tuna, M. Bodensteiner, R. E. P. Winpenny and R. A. Layfield, *Organometallics*, 2013, 32, 1224–1229.

23 N. F. Chilton, D. Collison, E. J. L. McInnes, R. E. P. Winpenny and A. Soncini, *Nat. Commun.*, 2013, 4, 2551–2553.

24 (*a*) S.-S. Liu, L. Xu, S.-D. Jiang, Y.-Q. Zhang, Y.-S. Meng, Z. Wang, B.-W. Wang, W.-X. Zhang, Z. Xi and S. Gao, *Inorg. Chem.*, 2015, 54, 5162–5168; (*b*) Y.-S. Meng, S.-D. Jiang, B.-W. Wang and S. Gao, *Acc. Chem. Res.*, 2016, 49, 2381–2389.

25 (*a*) S. K. Langley, D. P. Wielechowski, V. Vieru, N. F. Chilton, B. Moubaraki, L. F. Chibotaru and K. S. Murray, *Chem. Sci.*, 2014, 5, 3246–3256; (*b*) J. D. Rinehart, M. Fang, W. J. Evans and J. R. Long, *Nat. Chem.*, 2011, 3, 538; (*c*) N. Ahmed, C. Das, S. Vaidya, S. K. Langley, K. S. Murray and M. Shanmugam, *Chem. – Eur. J.*, 2014, 20, 14235–14239.

26 L.-Y. Xu, J.-P. Zhao, T. Liu and F.-C. Liu, *Inorg. Chem.*, 2015, 54, 5249–5256.

27 (*a*) G. Lorusso, J. W. Sharples, E. Palacios, O. Roubeau, E. K. Brechin, R. Sessoli, A. Rossin, F. Tuna, E. J. L. McInnes, D. Collison and M. Evangelisti, *Adv. Mater.*, 2013, 25, 4653–4656; (*b*) M. Evangelisti, O. Roubeau, E. Palacios, A. Camon, T. N. Hooper, E. K. Bre-chin and J. J. Alonso, *Angew. Chem., Int. Ed.*, 2011, 50, 6606–6609.

28 A. Upadhyay, C. Das, M. Shanmugam, S. K. Langley, K. S. Murray and M. Shanmugam, *Eur. J. Inorg. Chem.*, 2014, 4320–4325.

29 A. Upadhyay, N. Komatireddy, A. Ghirri, F. Tuna, S. K. Langley, A. K. Srivastava, E. C. Sañudo, B. Moubaraki, K. S. Murray, E. J. L. McInnes, M. Affronte and M. Shanmugam, *Dalton Trans.*, 2014, 43, 259–266.

30 (*a*) Y. Z. Zheng, M. Evangelisti, F. Tuna and R. E. P. Winpenny, *J. Am. Chem. Soc.*, 2012, 134, 1057–1065; (*b*) Y.-C. Chen, J. Prokleš̆k, W.-J. Xu, J.-L. Liu, J. Liu, W.-X. Zhang, J.-H. Jia, V. Sechovsky and M.-L. Tong, *J. Mater. Chem. C*, 2015, 3, 12206–12211.

31 (*a*) I. A. Gass, E. K. Brechin and M. Evangelisti, *Polyhedron*, 2013, 52, 1177–1180; (*b*) M.-J. Martínez-Pérez, O. Montero, M. Evangelisti, F. Luis, J. Sesé, S. Cardona-Serra and E. Coronado, *Adv. Mater.*, 2012, 24, 4301–4305.

32 N. V. Dubrovina, V. I. Tararov, A. Monsees, R. Kadyrov, C. Fischera and A. Börner, *Tetrahedron: Asymmetry*, 2003, 14, 2739–2745.

33 (*a*) *SAINTSoftware Reference manuals, Version 6.45*, Bruker Analytical X-ray Systems, Inc., Madison, WI, 2003; (*b*) G. M. Sheldrick, *SHELXS-97, Program for Crystal StructureSolution*, University of Göttingen, Göttingen, Germany, 1997; (*c*) G. M. Sheldrick, *Acta Crystallogr., Sect. A: Found. Adv.*, 2015, 71, 3–8; (*d*) G. M. Sheldrick, *Acta Crystallogr., Sect. C: Struct. Chem.*, 2015, 71, 3–8.